The phyto-bacterioplankton couple in a shallow freshwater ecosystem: Who leads the dance?

Imen Louati, Naoise Nunan, Kevin Tambosco, Cécile Bernard, Jean-François Humbert, Julie Leloup

Highlights

- High frequency monitoring of phytoplankton and bacterioplankton dynamics in an eutrophic shallow lake
- Phytoplankton and associated bacterioplankton communities can be seen as a couple in interaction but with flexible species variations
- Free-living bacterioplankton is under less direct influence of the phytoplankton communities and environmental variables dynamics

The phyto-bacterioplankton couple in a shallow freshwater ecosystem: who leads the dance?

Authors : Imen Louati[1], Naoise Nunan[1,3], Kevin Tambosco[1], Cécile Bernard [2], Jean-François Humbert[1], and Julie Leloup[1].

Affiliations :

1) UMR 7618 iEES-Paris Sorbonne Université - 4 place Jussieu - 75252 Paris Cedex 05 - France

2) UMR 7245 MCAM Muséum National d'Histoire Naturelle - CNRS, CP 39, 12 rue Buffon,75231 Paris Cedex 05, France

3) Department of Soil and Environment, Swedish University of Agricultural Sciences, P.O. Box 7014, 75007 Uppsala, Sweden

Corresponding author : Julie Leloup

UMR 7618 iEES-Paris Sorbonne Université - 4 place Jussieu - 75252 Paris Cedex 05 - France

Phone : 0033 144 273 826

E-mail : jleloup@sorbonne-universite.fr

Keywords / Highlights

- High frequency monitoring of phytoplankton and bacterioplankton dynamics in an eutrophic shallow lake
- Phytoplankton and associated bacterioplankton communities can be seen as a couple in interaction but with flexible species variations
- Free-living bacterioplankton is under less direct influence of the phytoplankton communities and environmental variables dynamics

Abstract

Bloom-forming phytoplankton dynamics are still unpredictable, even though it is known that several abiotic factors, such as nutrient availability and temperature, are key factors for bloom development. We investigated whether biotic factors, i.e. the bacterioplankton composition (via 16SrDNA metabarcoding), were correlated with phytoplankton dynamics, through a weekly monitoring of a shallow lake known to host recurrent cyanobacterial blooms. We detected concomitant changes in both bacterial and phytoplankton community biomass and diversity. During the bloom event, a significant decrease in phytoplankton diversity, was detected, with a first co-dominance of *Ceratium*, *Microcystis* and *Aphanizomenon*, followed by a co-dominance of the two cyanobacterial genera. In the same time, we observed a decrease of the particle-associated (PA) bacterial richness and the emergence of a specific bacterial consortium that was potentially better adapted to the new nutritional niche. Unexpectedly, changes in PA bacterial communities occurred just before the development the emergence of the phytoplanktonic bloom and the associated modification of the phytoplanktonic community composition, suggesting that changes in environmental conditions leading to the bloom, were first sensed by the bacterial PA community. This last was quite stable throughout the bloom event, even though there were changes in the blooming species, suggesting that the association between cyanobacterial species and bacterial communities may not be as tight as previously described for monospecific blooming communities. Finally, the dynamics of the free-living (FL) bacterial communities displayed a different trajectory from those of the PA and phytoplankton communities. This FL communities can be viewed as a reservoir for bacterial recruitment for the PA fraction. Altogether, these data also highlight s that the spatial organization within these different microenvironments in the water column is a relevant factor in the structuring of these communities.

Keywords: cyanobacterial bloom, eutrophic lake, phototrophic-heterotrophic interactions, temporal dynamic

1. Introduction

Due to the health risks for human populations associated with cyanobacterial blooms, numerous studies have been published during the past 20 years on the determinism of these cell proliferations, their potential toxicity, as well as the diversity of metabolites they produce (e.g. Demay et al., 2019). Overall these studies have shown that cyanobacterial blooms are strongly associated with the eutrophication of lentic ecosystems (e.g. Smith, 2003; Heisler et al., 2008; Conley et al., 2009) and, more recently, that climatic change (temperature and light mainly) tends to amplify these proliferations, as reviewed by Chorus et al. (2021). Despite the numerous studies on the genetics, ecophysiology and toxicity of bloom-forming cyanobacteria, cyanobacterial dynamics (appearance, intensity and duration) remain poorly understood (Harke et al., 2016, Wilhelm et al., 2020). This is particularly important because cyanobacterial blooms are frequently characterized by chaotic population dynamics, with rapid population rises and declines (Pobel et al., 2011), but we do not have a clear understanding of the processes or interactions that underlie these dynamics.

A number of studies have shed a light on the role of biotic interactions as potential structuring factors in combination with environmental conditions. The competition between cyanobacteria and microalgae (e.g. Huisman et al., 1999; Ji et al., 2017; Wang et al., 2017) or the grazing of cyanobacteria by zooplankton (e.g. Dmitrieva and Semenova, 2011; Ka et al., 2012; Ger et al., 2016) are examples of such biotic interactions. It is only recently that the interactions occurring between cyanobacteria and the other bacteria have been investigated in freshwater ecosystems. These interactions are crucial as the recycling of organic matter (OM) produced by cyanobacteria

and other phytoplankton is performed by heterotrophic bacteria in the microbial loop (Cole et al., 1988). These bacteria are either planktonic in the water column (free-living - FL fraction) or associated with the immediate environment of phytoplanktonic cells (Particle-associated -PA fraction), thus forming the phycosphere where specialized interactions are expected to occur (Song et al., 2017; Zhang et al., 2021). The composition and diversity of these PA and FL communities are known to be significantly different (e.g. Parveen et al., 2013; Seymour et al., 2017). These differences are explained by the continuous input of autochthonous OM resulting from phytoplanktonic extracellular OM and cell lysis, which is more readily available to bacterial communities within the phycosphere, and which preferentially affects the metabolic capacities of PA communities relative to FL communities (Louati et al., 2015; Woodhouse et al., 2018; Hu et al., 2020). Moreover, the chemical composition of photosynthates varies both with the taxonomic composition of the phytoplankton and their physiological status. Labile low-molecular-weight molecules (such as amino acids and fatty acids) are produced during the growth phase and high-molecular-weight molecules (polysaccharides, proteins) during the senescence phase (Leloup et al., 2013; Buchan et al., 2014; Seymour et al., 2017; Camarena-Gómez et al., 2018, Lemoigne et al, 2021). Thus, the taxonomic composition of the phytoplankton, their growth state, as well as their physiological status can modulate the structure of the PA and FL bacterial communities, (e.g. Grossart et al., 2006; Zhu et al., 2016; Berg et al., 2018; Pascault et al., 2021). It has been suggested that the composition of bacterial communities could also modulate the metabolic interactions between heterotrophic bacteria and phytoplankton (Pinhassi et al., 2004; Grossart et al., 2006; Klindworth et al., 2014), and could lead to modifications of some phytoplanktonic traits, such as growth rate or aggregation capacity, and ultimately their fitness. For example, Jackrel et al. (2021) demonstrated that the presence of established associated bacterial species can facilitate the growth rates, environmental stress responses and fitness of green algae. Moreover, Jankowiac and Gobler

(2020) suggested that the metabolic activities, the growth rates and the diversity of both the phytoplanktonic and the bacterial communities, affected the acclimation rates of the phycosphere to changes in environmental conditions.

Based on these data, we hypothesized that the bacterial and phytoplanktonic communities could have synchronized seasonal dynamics, and that different phytoplankton-bacterioplankton couples would emerge depending on the environmental conditions. As recently emphasized, studies have been carried out over a limited range of spatial and temporal scales, and high frequency monitoring approaches in natural conditions are needed (Lindh et al., 2015; Jankowiac and Gobler, 2020). High frequency monitoring can provide a fine understanding of the dynamics of the associations between phytoplankton and bacterial communities. This is particularly true in small sized ecosystems where the phytoplankton communities display rapid and chaotic changes (Pobel et al., 2011). Such an approach could provide novel insights into processes occurring between bacteria and phytoplankton during different stages of a bloom event, or under different environmental conditions and their potential roles in bloom dynamics.

To explore these hypotheses, we monitored a shallow lake known to host recurrent cyanobacterial blooms on a weekly basis in order to determine (i) whether the dynamics of associated (PA) and free-living (FL) bacterial communities were synchronized with that of phytoplankton community (eukaryotic algae and cyanobacteria) dynamics or whether there was a lag between the two, (ii) whether the reduced phytoplankton diversity that is commonly observed during cyanobacterial blooms results in a concomitant reduction of either the PA or FL bacterial diversity and (iii) whether changes in bacterial communities composition was accompanied with the emergence of some specific potential functions during the bloom season, thus contributing to a better understanding of this process.

2. Experimental procedures

120 2.1. Study sites, sampling and fraction separation

121 The sampling site is a recreational lake located near the city of Champs-sur-Marne (Seine-et-
122 Marne, Ile-de-France, France, 48° 51'47.0 N, 02°35'53.9 E). This aquatic ecosystem has a surface
123 area of 0.1 km^2 with an average depth of 2.70 m, and, since 2006, it has experienced several
124 cyanobacterial bloom episodes (Ledreux et al., 2010). In 2013, a time-series sampling campaign
125 was performed in which weekly samples were collected from surface water (between 0.5 to 1m
126 depth) starting June 26th to October 28th (14 dates, July 1st and July 15th were not sampled), as
127 recommended for small lakes (Pobel et al., 2011). Triplicate raw water samples (50 to 100 mL
128 depending on the Chl-*a* content) were filtered through a 1.2 µm polycarbonate filter (Isopore
129 Membrane Millipore) to concentrate the particle-associated fraction (PA), followed by a 0.2 µm
130 polycarbonate filter (Nuclepore Polycarbonate - Whatman) in order to concentrate the free-living
131 fraction (FL). Filters were immediately frozen in liquid nitrogen and stored at -80°C until DNA
132 extraction. In parallel, raw water samples (2 L for Chl-*a* content and 150 mL for nutrient analysis)
133 were filtered in triplicate through a 0.7µm glass fiber filter (GFF - Whatman) pre-combusted at
134 450°C overnight. The filters and half of the eluates (collected in sterile polyethylene flasks) were
135 stored at -20°C. The remaining half of the eluates were preserved with 36 µl 85% phosphoric acid
136 (H_3PO_4) and stored at ambient temperature and in the dark, until physico-chemical measurements
137 were carried out.

138 2.2. Chlorophyll-*a* and phytoplankton analyses

139 Chlorophyll-a (Chl-*a*) content, which provides an estimation of the phytoplankton biomass, was
140 extracted and measured, in triplicate, by spectrophotometry after cell lysis (Demay et al., 2019).
141 Taxonomic identification (at the genus level) and total counts were performed on at least 400
142 phytoplankton units (cells, trichomes, and colonies), under a Nikon Eclipse TS-100 inverted
143 microscope (400X) (Table S1). The phytoplankton were characterized (at the genus level, Table

S2) in samples fixed in buffered formaldehyde (5% v/v), using taxonomic guides and keys based on morphological characteristics, as described in Talling (1986) and Cronberg and Annadotter (2006). The volume of each genus was either estimated using geometric shapes, as described by Sun and Liu (2003), taken from the Ile de France phytoplankton check list (Escalas et al., 2019) or, for rare genera, from the HELCOM phytoplankton check list (Olenina et al., 2006).

2.3. Physico-chemical analysis

Dissolved organic and inorganic N and P were determined in duplicate using an automated colorimetric procedure as described by Holmes et al. (1999), at the MIO-PACEM analytical platform (https://www.mio.osupytheas.fr/fr/plateformes-de-recherche/ptf-analytique-de-chimie-des-environnements-marins-pacem). Dissolved organic carbon (DOC) concentration was measured on a Shimadzu TOC VCSH analyzer, as in Rochelle et al. (2014). Meteorological data (temperature, rainfall and global radiation) were obtained from the Météo-France database (Meteo-France, Vincennes, France). All abiotic data are summarized in Table S3.

2.4. DNA extraction

DNA was extracted from a total of 84 filters (triplicate filters per date and per filter pore size, Table S4) following Louati et al. (2015). Briefly, each filter was flash-frozen in liquid nitrogen, and then transferred to Lysing Matrix E tubes (MP Biomedicals, Illkirch, France) with 1.1 mL of lysis buffer (40mM EDTA, 50mM Tris-HCl, 0.75 M sucrose). Bead-beating was applied for 3x30 sec at a speed of 6.5 m. s^{-1} (FastPrep1-24, MP Biomedicals, France). Lysozyme (0.6 mg. mL^{-1}) was then added to the filters and incubated at 37°C for 45 min with gentle stirring. Subsequently, sodium dodecyl sulfate (1% final concentration) and proteinase K (Thermo Scientific, France) were added, and incubated at 55°C for at least 90 min. Filter-debris were pelletized by centrifugation at 14 000 g for 5 min and supernatants were collected and purified twice with phenol-chloroform-isoamyl alcohol. After precipitation with sodium acetate (0.1 vol) and cold isopropanol (0.6 vol), the nucleic

acids were washed with 70% ethanol, and then re-suspended in 100 µL milliQ water. The DNA was stored at -20°C until analysis.

2.5. Quantification of total bacterial abundances

Total bacterial abundances were quantified by qPCR using primers targeting the 16S rDNA, N_2-fixing bacteria with primers targeting *nif*H gene, and denitrifying bacteria with primers targeting *nir*K and *nir*S genes, as described previously (Leloup et al., 2018). Reactions were carried out in a CFX96 Real Time PCR detection system (Bio-Rad, Marnes la Coquette, France) with a 20 µL reaction volume containing SsoAdvanced™ Universal SYBR® Green Supermix (Bio-Rad, Marne la Coquette, France), 1 mM of each primer, 2 µM bovine serum albumin and 0.4 ng and 4 ng of DNA (in order to detect amplification inhibition). Two quantitative PCR assays were performed and gene abundances were determined in duplicate. Standard curves were obtained using serial dilutions of linearized plasmids containing the studied genes respectively amplified from *Pseudomonas fluorescens* (16SrDNA sequences), *Azotobacter vinelandii* (*nif*H sequence), *Sinorhizobium meliloti (nir*K sequence*)*, and *Pseudomonas stutzeri* (*nir*S sequence).

2. 6. High-throughput sequencing

In order to exclude chloroplast and cyanobacterial sequences of the 16S rRNA fragment, the primer set 895F and 1492R, designed by Hodkinson and Lutzoni (2009), was used to amplify the V6-V8 region, as previously described in Louati et al. (2015). *In silico* analyses showed that most of cyanobacterial 16S rDNA sequences were excluded when using these primers (Louati et al., 2015). PCR amplification was performed in triplicate and pooled, as described in Louati et al. (2015). Briefly, DNA was amplified using the Phire Hot Start II DNA Polymerase (ThermoScientific, France) with a touchdown round (without TAG): 98°C for 3 min; 24 cycles of 98°C for 30 s, 65 to 55°C for 30 s with -0.4°C/cycle, 72°C for 60 s; followed by 12 cycles at 55°C and a final extension of 10 min at 72°C. A second PCR round was used to insert the TAG-primers within the sequences

192 at an annealing temperature of 55°C. The triplicate PCR products were pooled and purified using
193 MinElute Gel Extraction Kit (Qiagen, Valencia, CA). Pyrosequencing, using a Roche 454 GS-FLX
194 system (Titanium Chemistry), was performed by Eurofins - GATC (Konstanz, Germany). A total
195 of 84 PCR samples (14 dates, 2 fractions and 3 replicates) were sequenced.

196 2.7. Bioinformatic analysis

197 Nine of the 84 samples (FL_2207R2, FL_0209R2, FL_1609R3, FL_2810R1, FL_0508R1,
198 PA_2406R1, PA_CSM0807R1, PA_CSM0508R1, PA_CSM1208R1) were removed from the
199 dataset due to low (<1000) read content. Data were processed through the FROGS pipeline (Find
200 Rapidly OTU with Galaxy Solution) implemented on a galaxy instance (2.3.0)
201 (https://galaxy.migale.inra.fr/) (Escudié et al., 2018). First, raw data were cleaned according to size
202 criteria (500 to 600 bp) and homopolymer detection: all sequences with at least one homopolymer
203 of more than seven nucleotides and with a distance of less than or equal to 10 nucleotides between
204 two poor quality positions, i.e. with a Phred quality score below 10 (here 454 data), were removed.
205 After the prep-process, a total of 519 943 high quality reads were analyzed (Table S4). Reads were
206 clustered using the SWARM algorithm (2.1.5) that uses a local clustering threshold, by clustering
207 nearly identical amplicons iteratively with an aggregation distance of 1, as recently recommended
208 (Mahé et al., 2014). Within an OTU, the "consensus" sequence that will be used for assignment, is
209 the sequence that is the most abundant in the OTU (see Escudié et al., 2018). Chimera were then
210 removed using VSEARCH (Rognes et al., 2016). The low abundance OTUs (< 5 reads) were
211 removed from the dataset (Filtering step). At the sample level, datasets were rarefied to the lowest
212 number of reads. The taxonomic assignation of each cluster was carried out using the blast+ tool
213 (Camacho et al., 2009) against the SILVA 138-16S pintail 100 database (Pruesse et al., 2007),
214 which finds an alignment between each OTU seed (the most abundant sequence within the OTU)
215 and the database. Only the best hits with the same score are reported, and if several blast results

returned identical scores for an OTU, the taxonomy was determined for each hit at each taxonomic level. The blast scores (% identity, % coverage, length alignment, and e-value) for the first 100 OTUs in the dataset are provided in Table S5. For the rest of the OTUs (representing less than 0.01% of the abundance of the dataset), the weaker values detected were 78,837% of identity, 81,69% of query coverage and an e-value of $3.93.10^{-19}$. If these taxonomies differ across hits, the first level of conflict and all lower ones were set to 'Multi-affiliation'. After a multiple alignment using Mafft, a rooted phylogenetic tree was created with the FastTree and Phangorn R packages

2.8. Statistical analysis

All statistical analyses were performed using R (4.1.2, and 3.3.6) (R Development Core Team, http://www.R-project.org), and are listed in the supplemental file_2. The Phyloseq (1.36.0, McMurdie and Holmes, 2013) and Microbiome (1.14.0) packages were used to describe community composition and diversity. Cyanobacterial reads that remained in the dataset, were removed using the phyloseq function 'subset_taxa" (Table S1). Plots were drawn using the packages ggplot2 (3.3.5, Wickham, 2016) and Phyloseq. In order to identify significant groupings (*P*-value of 0.05 and 1000 permutations) in both the phytoplanktonic and bacterioplanktonic communities, SIMPROF analyses (similarity profiling with no *a priori*, Clustsig package 1.1, Clarke et al., 2008) were performed, based on the Bray-Curtis distance matrix (after a square-root transformation for the phytoplankton data). Three temporal stages were thus detected for the phytoplanktonic as well as for the bacterioplanktonic PA communities (see figure S1).

Richness (number of OTU), evenness (Pielou) and diversity (Simpson) indices were calculated. The relationships between these indices and environmental variables were identified using multivariate generalized additive models (GAM). Prior to model fitting, all candidate variables were tested for collinearity using Spearman's correlation analysis. Model were calculated using the gam() function of the mgcv package (Wood, 2011). Model selection was carried out using

the "select = TRUE" argument in the gam() function. Non-normal variates were log-transformed prior to analysis in or order to avoid attributing excessive weight to outliers.

A metrical dimensional scaling (MDS), based on the Bray Curtis distance matrix, was used for the ordination of the bacterioplankton communities. Differences according to the temporal stages (described above), as well as according to the fractions (PA and FL), were statistically tested using permutational PERMANOVA (9999 permutations), with ADONIS (vegan 2.6.2, Oksanen et al., 2022). Relationships between bacterial community structure and environmental variables were explored by a constrained correspondence analysis (vegan 2.6.2, Oksanen et al., 2022). Variance partitioning was measured based on the OTU table, a biotic table (Phytoplankton biomass and composition, bacterial and functional abundances), and an abiotic table (see Tables S1 and S3), using the varpart function (vegan 2.6.2, Oksanen et al., 2022). As the quantitative data have different units, data were transformed prior to analysis.

We then sought to identify the OTUs that contributed the most to the dissimilarity among communities using the SIMPER function (vegan 2.6.2, Oksanen et al., 2022) with the criterion of up to 70% of the cumulative explained dissimilarity (with an adjusted p-value < 0.1).

Two separated analyses were performed and illustrated as heatmaps:

i) the OTUs responsible for the dissimilarities between PA and FL communities, whatever the temporal stages, were identified. After a differential expression analysis (padj < 0.01, Table S7), three expression patterns were detected: up in the PA fraction, up in the FL fraction, or equally abundant in both (termed "cosmopolitan").

ii) the OTUs responsible for the dissimilarities between each three temporal stages, were identified within: a) the PA fraction and b) the FL fraction. A differential expression analysis of these OTUs was performed using DESeq2 (1.32.0, Love et al., 2014, padj < 0.01, Tables S8). Three expression patterns were identified: up in the Stage I, up in the stage II and up in the stage III.

2.9. Nucleotide read accession numbers

The nucleotide reads determined in this study have been deposited to the SRA database under the Project accession number: PRJNA579262 (https://www.ncbi.nlm.nih.gov/bioproject/).

3. Results

Strong temporal variations were observed in the composition and biomass of the phytoplankton community during the monitoring period (Figure 1). Based on a SIMPROF analysis, three temporal stages were distinguished:

(i) **Stage I** (06/24 and 07/08 - Phyto_Cluster_1 - Figure S1) was characterized by low biomass values and a large co-dominance of the phytoplankton community by Chlorophyta and Diatomophyta (Tables S1 and S2).

(ii) **Stage II** (07/22 to 08/26 - Phyto_Cluster_2 - Figure S1) was characterized by an increase of the biomass (with a max of 115 µg Chl-*a*. L^{-1} in mid-August) and by changes in the composition of the phytoplankton community, with a diversified mix of Dinophyta, Bacillariophyta, Euglenophyta, Chlorophyta, and Cyanobacteria (Tables S1 and S2) and a shift from a dominance by cyanobacteria (mainly belonging to *Dolichospermum* genus) at the beginning of this stage toward a dominance by Chlorophyta at the middle of the stage and finally a co-dominance by Chlorophyta and Dinophyta (mainly *Ceratium* genus) at the end of the stage II.

(iii) **Stage III** (09/02 to 10/28 - Phyto_Cluster_3a, b and c - Figure S1) was characterized by higher biomasses (with a max of 332 Chl-*a*. L^{-1} reached at beginning of September) and by a co-dominance of the phytoplankton community by *Ceratium* spp (Dinophyta) and Cyanobacteria until middle September, followed by a dominance by two cyanobacterial genera, *Microcystis* and *Aphanizomenon* (Tables S1 and S2).

As for the phytoplankton communities, a clustering in three stages was detected for the bacterial communities of the PA fraction (SIMPROF, $p < 0.05$, Figure S2). During the stage III, the same clustering in three subgroups found for the phytoplanktonic communities (Figure S1) was also observed for the PA-bacterial community (Figure S2). Interestingly, one discrepancy was detected for the sampling date of 26/08 (transition between the phytoplanktonic stages II and III, Figure 1), the PA-bacterial communities was clustering with the ones of the stage III (Figure S2, Bac_Cluster_3d), while the phytoplanktonic community was clustering with the ones of the stage II (Figure S1, Phyto_Cluster_2). No clustering was found for the FL communities.

Both the phytoplankton biomass (estimated by Chl-*a* values) and the PA bacterial abundances increased during the stages II and III with higher values during the bloom event (Figure 1 and S3). These increases were concomitant with a decrease in phosphate and dissolved organic P (DOP) and an increase of particulate organic P (POP) (Table S6). During the stage II, a peak of the N_2-fixing abundances was detected in the PA fraction, in correlation with temperature and nitrate (linear curve) and ammonium (exponential-shaped curve) (Table S3), followed by a peak of denitrifying bacteria at the beginning of the stage III in the PA and the FL fractions (Figure S3). The bacterial community structure was explored through richness and diversity indexes (Figure 2). In the PA fraction, all three indexes were lower during the stage III, while only a decrease of richness was observed in the FL fraction, during the stage II (Figure 2), and were correlated with phosphate, DOP, POP and temperature (Table S6). In the FL fraction, Richness was positively correlated to phosphate, and the Simpson and Evenness were both positively related to DOP and POP (Table S6).

The relationship between bacterial community structure and the biotic and abiotic variables was further explored with a redundancy analysis (Figure 3). First, the bacterial communities were clustered according to their lifestyle (PA vs FL, axis 1 and 2; 20.50 and 8.15%, p-value <0.001).

Second, the temporal dynamic was clearly highlighted for the PA fraction with the three stages being strongly separated (also detected in Figure S6). The PA-bacterial communities from the transition date (between stage II and III, 26/08) were the exception as previously highlighted in the Figure S2. This differentiation between stages was mainly due to higher cyanobacterial abundance, chl-*a* and DOC, DOP and POP concentrations during stage III, while the stage II was related to the presence of the Chlorophyta. In the FL fraction, the temporal dynamic was also detected but was less marked, and driven mainly by the temperature, and the phosphate and ammonium concentrations. A variance partitioning analysis showed that 16 to 18% of the total variance was explained by the abiotic data, and 39 to 44% by the biotic data (Figures S4).

Gammaproteobacteria always dominated the PA communities (78 to 97%) while Gammaproteobacteria and Actinobacteria were both dominant in the FL communities (from 20 to 80%, Figure S5A). We explored the dissimilarity between the PA and the FL communities with a selected dataset of 14 OTUs (SIMPER analysis, Figure 4 and Table S7). These OTUs displayed clear statistically significant (p-value<0.01) between each fraction: a set of seven OTUs (upper part) belonging to Micrococcales, Xanthomonadales and Burkholderiales, were higher in the FL fraction, while a set of seven OTUs (below part), belonging to the Burkholderiales and Rhodobacterales, were higher in the PA fraction (Figure 4). Thus, the differences between the communities within each fraction was mainly explained by a few OTUs that belonged to a few specific taxonomic families.

Within each fraction, the relative abundances of bacterial families differed between phytoplankton bloom stages (Figure S5B). In the PA community, the Burkholderiaceae were abundant during stages I and II, and the Nitrosomonadaceae during the stage III (Gammaproteobacteria). In the FL fraction, the Burkholderiaceae and Methylophilaceae were the major families, and the Nitrosomonadaceae also appeared during the stage III (Figure S5B). In

335 order to better understand the fine dynamics of these bacterial families, the trajectories of the OTUs
336 explaining most of the dissimilarity between the temporal stages, for each fraction separately, was
337 explored and presented in Figures 5.

338 Thirty-one and twenty-one OTUs (in the PA and FL fractions, respectively) displayed clear
339 statistically significant ($P<0.01$) dynamics according to the three stages (Table S8). In the PA
340 fraction, thirteen and twelve OTUs were respectively over-represented during stages I and II. These
341 OTUs were affiliated mostly to the Burkholderiales, followed by Aeromonadales,
342 Methylococcales, Enterobacterales, Rhodobacterales and Halothiobacillales. Only six OTUs
343 belonging to Burkholderiales, principally Nitrosomanadaceae were over-represented during stage
344 III. It is worth noting that these six OTUs were already present and abundant at the transition date
345 (August 26, dashed square, Figure 5A) where the phytoplankton was co-dominated by *Ceratium*
346 spp and Chlorophyta.

347 In the FL fraction, the picture was different, a smaller number of OTUs (4 to 7) were
348 overrepresented, but were assigned to a higher number of bacterial families and orders than the PA
349 fraction (Table S8), also in the stage III (Figure 5B). Interestingly, some OTUs were both
350 highlighted in the PA and FL fractions but not during the same stage. The OTU 1 was over-
351 represented in both PA and FL fractions during the stage III. The OTUs 6 and 9, were found to be
352 cosmopolitan in the FL fraction, but over-represented in the PA fraction during the stage I and
353 almost inexistent in the stage III.

354

355 **4. Discussion**

356 Although numerous studies of phytoplanktonic blooms have been carried out throughout
357 the world, especially focused on cyanobacterial blooms, the interactions that underlie bloom
358 dynamics (appearance, intensity and duration) remain poorly understood (e.g. Wilhelm et al.,

2020). In particular, it has been argued that a better description of the relationships between phytoplankton and their associated bacteria within the phycosphere is necessary. Therefore, we carried out a weekly-monitoring of a small French shallow lake throughout a bloom season in order to better understand the fine dynamics of phytoplankton and bacterioplankton communities. As previously observed in this lake (Ledreux et al., 2010, Louati et al., 2015), the phytoplankton biomass increased during the summer and was accompanied by a decrease in phytoplankton taxa richness during the cyanobacterial bloom. Concomitantly, a decrease of phosphate concentration was observed, most likely related to the high cellular growth that is typical of bloom events and the associated high P demand for ribosome and protein production (Elser et al, 2020, Pascault et al., 2021). This could indicate a shift in the available P forms towards particulate organic P (Nalven et al. 2020). The N concentrations remained high throughout the period of the survey. This can be explained by the presence of two N_2-fixing cyanobacterial genera, *Dolichospermum* associated with Chlorophyta in July during the first peak of phytoplankton biomass (stage II, Chl-*a* level of 110 µg. L^{-1}), and *Aphanizomenon* associated with *Microcystis* during the second intense bloom (Stage III, Chl-*a* level up to 332 µg. L^{-1}). These dynamics, showing temporal succession of N_2-fixing and non N_2-fixing cyanobacteria as well as co-dominance, are frequently observed in eutrophic ecosystems during the summer period (Beversdorf et al., 2013; Louati et al., 2015). Within such cyanobacterial co-dominance, the bacterial interactions promote nutrient exchanges and recycling in order to face the high nutrient demand, as observed by Pascault et al. (2021), where mineral N (newly fixed and/or allochthonous) was preferentially transformed into amino acids for the growth of cyanobacteria and their associated microbiome. It thus suggests that the input of newly formed N by the N_2-fixing cyanobacteria promotes the growth and emergence of *Microcystis* cells by supplementing the N stock (Jackrel et al., 2021; Pascault et al., 2021).

382 All the changes in the phytoplankton community were accompanied by substantial changes
383 in the PA communities. In particular, the bacterial communities of the stage III were clearly
384 different from those of the stages I and II. These changes were underscored by an increase of the
385 bacterial abundances as well as a strong decrease in the richness and diversity indexes during the
386 bloom event. Within the phycosphere, most of the interactions are believed to be driven by the
387 recycling of dissolved organic matter (DOM), and can be modulated by DOM quantity and quality
388 (Amin et al., 2015 Zhang et al., 2019), by the composition of the daily extracellular phytoplankton
389 production (EPP, Landa et al., 2014, Park et al., 2022) and by microbial senescence/predation
390 (Simek et al., 2008; Seymour et al., 2017). The strong increase in phytoplanktonic OM during the
391 bloom event, likely led to the reduction of the microbial diversity and changes in composition, with
392 species that are well adapted to the new nutritional niche coming to dominate and to a competitive
393 exclusion of other species (Teeling et al., 2012, Luria et al., 2016; Nelson et al., 2021). In this
394 context, we observed the emergence of Nitrosomonadaceae and Comamonadaceae known to be
395 potential nitrifying and denitrifying microorganisms, during the bloom in the PA fraction. They
396 have been previously detected in several cyanobacteria and dinoflagellates blooms (Louati et al.,
397 2015; Nelson et al., 2021; Pascault et al., 2021, Fortin et al., 2022), and might ensure a tight
398 recycling of N during bloom events, as they occur concomitantly with N_2-fixing cyanobacteria.
399 Nevertheless, their relative contribution to the N cycle has not yet been quantified (Kolmonen et
400 al., 2004).

401 Here, the weekly monitoring has also highlighted that the PA bacterial communities in the
402 stage III were very close to the communities observed at the transition date (stage II - August 26).
403 At this time there was an increase in the biomass of *Ceratium spp* in the phytoplankton community.
404 Moreover, the structure of PA communities was stable during all the stage III, even after the
405 replacement of *Ceratium* by the cyanobacteria. These data show that the bacterial communities

406 associated with *Ceratium* and the co-dominant cyanobacteria, *Microcystis* and *Aphanizomenon*,
407 had similar compositions. *Ceratium*, a mixotrophic dinoflagellate, is able to reach high biomasses
408 in eutrophic ecosystems and has shown seasonal dynamics that are similar to those of cyanobacteria
409 in these ecosystems (Gligora *et al*., 2003; Grigorszky et al., 2019). All these findings suggest that
410 environmental conditions leading to the genesis of a phytoplankton bloom during stage III have
411 resulted in the selection of a stable PA-bacterial community during all the bloom process (from its
412 early development to its end), even if there were changes in the blooming species. These results
413 bring new insight into phytoplankton-bacteria interactions, with previous studies detecting specific
414 bacterial consortium within monospecific phycosphere (Louati et al, 2015, Cook et al., 2020,
415 Gobler and Jankowiak, 2022). The couple formed by phytoplanktonic species and their associated
416 bacteria are often viewed as an interactome which is selected by the abiotic conditions. Here, the
417 weekly sampling during the summer phytoplankton succession has uncovered the possibility that
418 the association between cyanobacterial species and bacterial communities may not be as tight as
419 observed for monospecific blooming communities, and that environmental conditions are likely to
420 play a very important role in the interactions between phytoplankton and bacteria. The bloom event
421 was constituted of several eukaryotic and bacterial photosynthetic species, most certainly leading
422 to a composite of extracellular phytoplanktonic OM resources, that might have selected and
423 ensured that a more stable bacterial community, present for several weeks during the bloom event,
424 occurred. Finally, we can hypothesize that the bacterial signature in the PA may be indicative of
425 an early bacterial community response to environmental changes, that are sensed later by the
426 phytoplanktonic species. Changes in the associated bacterial communities would thus be beneficial
427 for the development and the severity of the phytoplanktonic bloom. Within the phyto-
428 bacterioplankton couple, the latter are often underestimated as well as their role in the emergence
429 of bloom. However, these theories need to be tested experimentally in the lab.

The highly dynamic changes in the phytoplanktonic community can be seen as short-term pulses of disturbances (via the releases of specific DOM), provoking resilience phenomena (rapid recovery) of the associated microbiomes (Baert et al., 2016, Gobler and Jankowiak, 2022). This is particularly true for the PA fraction where the bacteria are more tightly spatially related to the nutrient and energy sources, as is found in the rhizosphere in soil (Seymour et al., 2017). The spatial localization within these microenvironments in the water column may therefore be a relevant factor in the structuring of the microbiomes. The bacteria in the FL fraction displayed different trends, with a decrease of the richness and diversity during the stage II, suggesting that there were differently influenced by the phytoplankton dynamics. Even though the differences between PA and FL communities are frequently reported (Liu et al. 2019; Parveen et al. 2013; Cai et al. 2014), the underlying bacterial assembly mechanisms are not yet well known. They could be based both on host selection and/or stochastic effects (Kimbrel et al. 2019, Zhou et al. 2019). Our data show that a set of OTUs, that discriminate the temporal dynamic within the PA fraction, were also present in the FL fraction throughout the monitoring period. These OTUs were positively or negatively associated with the phytoplankton dynamics. Thus, the FL communities could be viewed as a reservoir for bacterial recruitment for the PA fraction evolving under phytoplankton stage, and could act as a buffering compartment for the fluctuating phytoplanktonic dynamics.

To conclude, we detected that both the phyto- and bacterioplankton compositions changed concomitantly during the survey, suggesting that they could be viewed as a microbial couple interacting fluctuating together throughout the seasons. We also detected a modification of the PA bacterial community just before the emergence of the bloom. This signature may be indicative of an early bacterial community response to physico-chemical or biological, as yet unidentified, signals that were sensed later by the phytoplanktonic species, and should to be further explored.

As between-species interactions impact their ability to coexist, our findings show that bacterial communities could have the potential to modulate phytoplanktonic species diversity and community composition. Until now, only the fitness of photosynthetic microorganisms in the face of environmental changes has been considered (Pound et al., 2021). The data presented here suggest that abiotic and biotic factors are acting on the concomitant selection of phyto- and bacterioplankton couples in interaction, also termed interactome, and known to provide functional capacities for bloom sustainability (Cook et al., 2020; Wilhelm et al., 2020). Thus, studying the impact of anthropogenic pressure on aquatic ecosystems should focus as much on the phytoplankton perturbations as the bacterioplankton and their interactions within the phycosphere.

Acknowledgements:

This study was funded by the PHYCOCYANO project in the Jeunes Chercheurs-Jeunes Chercheuses program of the French ANR (Agence Nationale de la Recherche; ANR-11-JSV7-014-01). L. Albaric and A. Roullot are thanked for access to the Champ-sur-Marne recreational area. We are grateful to the INRA MIGALE bioinformatics facility (MIGALE, INRA, 2018. Migale bioinformatics Facility, doi: 10.15454/1.5572390655343293E12) for providing help and support. Chemical analyses were performed at the iEES-Paris analytical platform (Y. Marcangeli) and at the MIO-PACEM analytical platform (P. Raimbault).

Data accessibility

Raw sequences were deposited to the SRA database and can be accessed under the Project accession number PRJNA579262. Supplementary information accompanies the manuscript.

Author contributions

J.L. designed the study. J.L., I.L. and K.T. collected the data. J.L., N.N., J.F.H. and C.B. analyzed the data. J.L., N.N., J.F.H. and C.B. wrote the manuscript.

ORCID

Julie Leloup: https://orcid.org/0000-0002-2777-284X

Naoise Nunan: https://orcid.org/0000-0003-3448-7171

Jean-François Humbert: https://orcid.org/0000-0002-1519-5651

Cécile Bernard : https://orcid.org/0000-0001-7032-3989

Conflict of interest

The authors declare that they have no conflict of interest.

References

- Amin, S.A., Hmelo, L.R., van Tol, H.M., Durham, B.P., Carlson, L.T., Heal, K.R., … Armbrust, E.V., 2015. Interaction and signaling between a cosmopolitan phytoplankton and associated bacteria. Nature 522(7554), 98-101. doi: 10.1038/nature14488
- Baert, J.M., De Laender, F., Sabbe, K., Janssen, C.R., 2016. Biodiversity increases functional and compositional resistance, but decreases resilience in phytoplankton communities. Ecology 97(12), 3433-3440. doi: 10.1002/ecy.1601
- Berg, C., Dupont, C.L., Asplund-Samuelsson, J., Celepli, N.A., Eiler, A., Allen, A E., … Ininbergs, K., 2018. Dissection of microbial community functions during a cyanobacterial bloom in the Baltic sea via metatranscriptomics. Front. Mar. Sci. 5, 55. doi: 10.3389/fmars.2018.00055
- Beversdorf, L.J., Miller, T.R., McMahon, K.D., 2013. The role of nitrogen fixation in cyanobacterial bloom toxicity in a temperate, eutrophic lake. PLoS ONE 8(2), e56103. doi: 10.1371/journal.pone.0056103

- Buchan, A., LeCleir, G.R., Gulvik, C.A., González, J.M., 2014. Master recyclers: features and functions of bacteria associated with phytoplankton blooms. Nat. Rev. Microbiol. 12(10), 686-698. doi: 10.1038/nrmicro3326
- Cai, H., Jiang, H., Krumholz, L.R., Yang, Z., 2014. Bacterial community composition of size-fractioned aggregates within the phycosphere of cyanobacterial blooms in a eutrophic freshwater lake. PLoS ONE **9**: e102879. doi: 10.3389/fmicb.2019.02202
- Camacho, C., Coulouris, G., Avagyan, V., Ma, N., Papadopoulos, J., Bealer, K., Madden, T.L., 2009. BLAST+: architecture and applications. BMC Bioinformatics 10(1), 421. doi: 10.1186/1471-2105-10-421
- Camarena-Gómez, M., Lipsewers, T., Piiparinen, J., Eronen-Rasimus, E., Perez-Quemaliños, D., Hoikkala, L., … Spilling, K., 2018. Shifts in phytoplankton community structure modify bacterial production, abundance and community composition. Aquat Micro. Ecol. 81(2), 149-170. doi: 10.3354/ame01868
- Chorus, I., Fastner, J., Welker, M., 2021. Cyanobacteria and cyanotoxins in a changing environment: concepts, controversies, challenges. Waters 13, 2463. doi: https://doi.org/10.3390/w13182463
- Clarke, K.R., Somerfield, P.J., Gorley R.N., 2008. Testing of null hypothesis in exploratory community analyses: similarity profiles and biota-environment linkage. J. Exp. Mar. Biol. Ecol. 366, 56-69. https://doi.org/10.1016/j.jembe.2008.07.009
- Cole, J., Findlay, S., Pace, M., 1988. Bacterial production in fresh and saltwater ecosystems: a cross-system overview. Mar Ecol Progr Series 43, 1-10. doi: 10.3354/meps043001

- Conley, D.J., Paerl, H.W., Howarth, R.W., Boesch, D.F., Seitzinger, S.P., Havens, K.E., ... Likens, G. E., 2009. Controlling eutrophication : nitrogen and phosphorus. Science 320, 1014-1015. doi: 10.1126/science.1167755
- Cook, K.V., Li, C., Cai, H., Krumholz, L.R., Hambright, K.D., Paerl, H.W., … Zhu, G., 2020. The global *Microcystis* interactome. Limnol. Ocean. 65(S1). doi: 10.1002/lno.11361
- Cronberg, G., Annadotter, H., 2006. Manual on aquatic cyanobacteria: a photo guide and a synopsis of their toxicology. ISSHA Eds, ISBN: 9788799082704.
- Demay, J., Bernard, C., Reinhardt, A., Marie, B., 2019. Natural Products from Cyanobacteria: Focus on Beneficial Activities. Mar. Drugs 17(6), 320. doi: 10.3390/md17060320
- Dmitrieva, O. A., Semenova, A.S., 2011. Seasonal dynamics of phyto- and zooplankton and their interactions in the hypereutrophic reservoir. Inland Wat. Biol. 4, 308-315. https://doi.org/10.1134/S1995082911030059
- Elser, J.J., Sterner, R.W., Gorokhova, E., Fagan W.F., Markow, T.A, …Weider, L.J., 2000. Biological stoichiometry from genes to ecosystems. Ecol. Lett. 3, 540-555. https://doi.org/10.1111/j.1461-0248.2000.00185.x
- Escalas, A., Catherine, A., Maloufi, S., Cellamare, M., Hamlaoui, S., … Bernard, C., 2019. Drivers and ecological consequences of dominance in periurban phytoplankton communities using networks approaches. Wat. Res. 163. https://doi.org/10.1016/j.watres.2019.114893
- Escudié, F., Auer, L., Bernard, M., Mariadassou, M., Cauquil, L., Vidal, K., … Pascal, G., 2018. FROGS: Find, Rapidly, OTUs with Galaxy Solution. Bioinformatics 34(8), 1287-1294. doi: 10.1093/bioinformatics/btx791

- Fortin, S.G., Song, B., Anderson, I.C., and Reece, K.S., 2022. Blooms of the harmful algae *Margalefidinium polykrikoides* and *Alexandrium monilatum* alter the York River Estuary microbiome. Harmful Algae 114, 102216. doi: 10.1016/j.hal.2022.102216
- Ger, K.A., Urrutia-Cordero, P., Frost, P.C., Hansson, L.A., Sarnelle, O., …Lürling, M., 2016. The interaction between cyanobacteria and zooplankton in a more eutrophic world. Harmful Algae 54, 128-144. doi: 10.1016/j.hal.2015.12.005
- Gligora, M., Plenković-Moraj, A., Ternjej, I., 2003. Seasonal distribution and morphological changes of *Ceratium hirundinella* in two mediterranean shallow lakes. Hydrobiol. 509, 213-220.
- Gobler, C. J., Jankowiak, J. G., 2022. Dynamic responses of endosymbiotic microbial communities within Microcystis colonies in north american lakes to altered nitrogen, phosphorus, and temperature levels. Front. Microbiol. 3890.
- Grigorszky, I., Gligora-Udovič, M., Gábor, B., 2019. Drivers of the *Ceratium hirundinella* and *Microcystis aeruginosa* coexistence in a drinking water reservoir. Limnetica 38, 41-53.
- Grossart, H.-P., Czub, G., Simon, M., 2006. Algae-bacteria interactions and their effects on aggregation and organic matter flux in the sea. Env. Microbiol. 8(6), 1074-1084. doi: 10.1111/j.1462-2920.2006.00999.x.
- Harke, M.J., Steffen, M.M., Gobler, C.J., Otten, T.G., Wilhelm, S.W., … Paerl, H.W., 2016. A review of the global ecology, genomics, and biogeography of the toxic cyanobacterium, *Microcystis* spp. Harmful Algae 54, 4-20. doi: 10.1016/j.hal.2015.12.007.
- Heisler, J., Glibert, P.M., Brukholder, J.M., Anderson, D.M., Cochlan, W., Dennison, W.C., … Suddleson, M., 2008. Eutrophication and harmful algal blooms: a scientific consensus. Harmful Algae 8, 3-13. doi: 10.1016/j.hal.2008.08.006

- Hodkinson, B.P., Lutzoni, F., 2010. A microbiotic survey of lichen-associated bacteria reveals a new lineage from the Rhizobiales. Symbiosis 49, 163-180. doi: 10.1007/s13199-009-0049-3
- Holmes, R.M., Aminot, A., Kérouel, R., Hooker, B.A., Peterson, B.J., 1999. A simple and precise method for measuring ammonium in marine and freshwater ecosystems. Can. J. Fish. Aqua. Sci. 56, 8. doi:10.1139/f99-128.
- Hu, Y., Xie, G., Jiang, X., Shao, K., Tang, X., Gao, G., 2020. The relationships between the free-living and particle-attached bacterial communities in response to elevated eutrophication. Front. Microbiol. 11, 423. doi: 10.3389/fmicb.2020.00423
- Huisman, J., Jonker, R.R., Zonneveld, C., Weissing, F.J., 1999. Competition for light between phytoplankton species: experimental tests of mechanistic theory. Ecology, 80, 211-222. doi : 10.1038/s41579-018-0040-1
- Jackrel, S.L., Yang, J.W., Schmidt, K.C., Denef, V.J., 2021. Host specificity of microbiome assembly and its fitness effects in phytoplankton. ISME J. 15(3), 774-788. doi: 10.1038/s41396-020-00812-x
- Jankowiak, J.G., Gobler, C., 2020. The composition and function of microbiomes within *Microcystis* colonies are significantly different than native bacterial assemblages in two north american lakes. Front. Microbiol. 11, 1016. doi: 10.3389/fmicb.2020.01016
- Ji, X., Verspagen, J.M.H., Stomp, M., Huisman, J., 2017. Competition between cyanobacteria and green algae at low versus elevated CO_2: who will win, and why? J. Exp. Bot. 68, 3815-3828. doi: 10.1093/jxb/erx226
- Ka, S., Mendoza-Vera, J.M., Bouvy, M., Champalbert, G., N'Gom-Ka, R., Pagano, M., 2012. Can tropical freshwater zooplankton graze efficiently on cyanobacteria? Hydrobiol. 679, 119-138. doi:10.1007/s10750-011-0860-8

- Kimbrel, J.A., Samo, T.J., Ward, C., Nilson, D., Thelen, M.P., Siccardi, A., …, Mayali, X. 2019. Host selection and stochastic effects influence bacterial community assembly on the microalgal phycosphere. Algal Research 40, 101489.
- Klindworth, A., Mann, A.J., Huang, S., Wichels, A., Quast, C., Waldmann, J., … Glöckner, F.O., 2014. Diversity and activity of marine bacterioplankton during a diatom bloom in the North Sea assessed by total RNA and pyrotag sequencing. Mar. Genomics 18, 185-192. doi: 10.1016/j.margen.2014.08.007
- Kolmonen, E., Sivonen, K., Rapala, J., Haukka, K., 2004. Diversity of cyanobacteria and heterotrophic bacteria in cyanobacterial blooms in Lake Joutikas, Finland. Aqu. Microb. Ecol. 36, 201-211. doi: 10.3354/ame036201
- Landa, M., Cottrell, M.T., Kirchman, D.L., Kaiser, K., Medeiros, P.M., Tremblay, L., …, Obernosterer, I., 2014. Phylogenetic and structural response of heterotrophic bacteria to dissolved organic matter of different chemical composition in a continuous culture study: bacterial diversity and dissolved organic matter. Environ. Microbiol. 16: 1668-1681. doi :10.1111/1462-2920.12242.
- Ledreux, A., Thomazeau, S., Catherine, A., Duval, C., Yéprémian, C., Marie, A., Bernard, C., 2010. Evidence for saxitoxins production by the cyanobacterium *Aphanizomenon gracile* in a french recreational water body. Harmful Algae 10(1), 88-97. doi: 10.1016/j.hal.2010.07.004
- Leloup, M., Nicolau, R., Pallier, V., Yéprémian, C., Feuillade-Cathalifaud, G., 2013. Organic matter produced by algae and cyanobacteria: quantitative and qualitative characterization. J. Env. Sciences 25(6), 1089-1097. doi: 10.1016/S1001-0742(12)60208-3

- Leloup, J., Baude, M., Nunan, N., Mériguet, J., Dajoz, I., Le Roux, X., Raynaud, X., 2018. Unravelling the effects of plant species diversity and aboveground litter input on soil bacterial communities. Geoderma 317:1-7. doi: https://doi.org/10.1016/j.geoderma.2017.12.018
- Lemoigne, D., Demay, J., Reinhardt, A., Bernard, C., Kim Tiam, S., Marie, B., 2021 Dynamics of the metabolome of *Aliinostoc* sp. PMC 882.14 in response to light and temperature variations. Metabolites 11(11), 745. doi: 10.3390/metabo11110745
- Lindh, M. V., Sjöstedt, J., Andersson, A. F., Baltar, F., Hugerth, L. W., Lundin, D., … Pinhassi, J., 2015. Disentangling seasonal bacterioplankton population dynamics by high-frequency sampling: high-resolution temporal dynamics of marine bacteria. Env. Microbiol. 17(7), 2459-2476. doi: 10.1111/1462-2920.12720
- Liu, M., Liu, L., Chen, H., Yu, Z., Yang, J.R., Xue, Y., … Yang, J., 2019. Community dynamics of free-living and particle-attached bacteria following a reservoir *Microcystis* bloom. Science Total Environ. 660, 501-511.
- Louati, I., Pascault, N., Debroas, D., Bernard, C., Humbert, J.-F., Leloup, J. (2015). Structural diversity of bacterial communities associated with bloom-forming freshwater cyanobacteria differs according to the cyanobacterial genus. PLoS ONE 10(11), e0140614. doi: 10.1371/journal.pone.0140614
- Love, M.I., Huber, W., Anders, S., 2014. Moderated estimation of fold change and dispersion for RNA-seq data with DESeq2. Gen. Biol. 15(12): 550.
- Luria, C.M., Amaral-Zettler, L.A., Ducklow, H.W., Rich, J.J., 2016. Seasonal succession of free-living bacterial communities in coastal waters of the western Antarctic peninsula. Front. Microbiol. 7. doi: 10.3389/fmicb.2016.01731

- Mahé, F., Rognes, T., Quince, C., de Vargas, C., Dunthorn, M., 2014. Swarm: Robust and fast clustering method for amplicon-based studies. PeerJ, 2, e593. doi: 10.7717/peerj.593
- McMurdie, P.J., Holmes, S., 2013. Phyloseq: an R package for reproducible interactive analysis and graphics of microbiome census data. PLoS ONE 8(4), e61217. doi: 10.1371/journal.pone.0061217
- Nalven, S.G., Ward, C.P., Payet, J.P., Cory, R.M., Kling, G.W., Sharpton, T.J., …, Crump, B.C., 2020. Experimental metatranscriptomics reveals the costs and benefits of dissolved organic matter photo-alteration for freshwater microbes. Environ. Microbiol. 22, 3505-3521. doi:10.1111/1462-2920.15121
- Nelson, C., Giraldo-Silva, A., Garcia-Pichel, F., 2021. A symbiotic nutrient exchange within the cyanosphere microbiome of the biocrust cyanobacterium, *Microcoleus vaginatus*. ISME J. 15(1), 282-292. doi: 10.1038/s41396-020-00781-1
- Oksanen, J., Simpson, G., Blanchet, F., Kindt, R., Legendre, P., Minchin, P., ... Weedon, J., 2022. Vegan: community ecology package. R package version 2.6-2, https://cran.r-project.org/web/packages/vegan/index.html.
- Olenina, I., Hajdu, S., Edler, L., Wasmund, N., Busch, S., Göbel, J., ... Niemkiewicz, E., 2006. Biovolumes and size-classes of phytoplankton in the Baltic Sea. Balt. Sea Environ. Proc. 106, 144pp. https://doi.org/HELCOM
- Park, J., Kim, G., Kwon, H.K., Han, H., Park, T.G., Son, M., 2022. Origins and characteristics of dissolved organic matter fueling harmful dinoflagellate blooms revealed by δ13C and d/l-Amino acid compositions. Sci Rep. 12, 15052.
- Parveen, B., Mary, I., Vellet, A., Ravet, V., Debroas, D., 2013. Temporal dynamics and phylogenetic diversity of free-living and particle-associated Verrucomicrobia communities in

relation to environmental variables in a mesotrophic lake. FEMS Microbiol. Ecol. 83(1), 189-201. doi: 10.1111/j.1574-6941.2012.01469.x

- Pascault, N., Rué, O., Loux, V., Pédron, J., Martin, V., Tambosco, J., … Leloup, J., 2021. Insights into the cyanosphere: capturing the respective metabolisms of cyanobacteria and chemotrophic bacteria in natural conditions? Env. Microbiol. Rep 13(3), 364-374. doi: 10.1111/1758-2229.12944
- Pinhassi, J., Sala, M.M., Havskum, H., Peters, F., Guadayol, Ò., Malits, A., Marrasé, C., 2004. Changes in bacterioplankton composition under different phytoplankton regimens. Appl. Env. Microbiol. 70(11), 6753-6766. doi: 10.1128/AEM.70.11.6753-6766.2004
- Pobel, D., Robin, J., Humbert, J.-F., 2011. Influence of sampling strategies on the monitoring of cyanobacteria in shallow lakes: lessons from a case study in France. Wat. Res. 45(3), 1005–1014. doi: 10.1016/j.watres.2010.10.011
- Pound, H.L., Martin, R.M., Sheik, C.S., Steffen, M.M., Newell, S.E., Dick, G.J., … Wilhelm, S.W., 2021. Environmental studies of cyanobacterial harmful algal blooms should include interactions with the dynamic microbiome. Envi. Sci. Tech. acs.est.1c04207. doi: 10.1021/acs.est.1c04207
- Pruesse, E., Quast, C., Knittel, K., Fuchs, B.M., Ludwig, W., Peplies, J., Glockner, F.O., 2007. SILVA: a comprehensive online resource for quality checked and aligned ribosomal RNA sequence data compatible with ARB. Nucl. Acids Res. 35(21), 7188-7196. doi: 10.1093/nar/gkm864
- Rochelle-Newall, E., Hulot, F.D., Janeau, J.L., Merroune, A., 2014. CDOM fluorescence as a proxy of DOC concentration in natural waters: a comparison of four contrasting tropical systems. Environ Monit Assess 186, 589-596.

- Rognes, T., Flouri, T., Nichols, B., Quince, C., Mahé, F., 2016) VSEARCH: a versatile open source tool for metagenomics. PeerJ 4, e2584. doi: 10.7717/peerj.2584
- Seymour, J.R., Amin, S.A., Raina, J.-B., Stocker, R., 2017. Zooming in on the phycosphere: The ecological interface for phytoplankton-bacteria relationships. Nature Microbiol. 2(7), 17065. doi: 10.1038/nmicrobiol.2017.65
- Simek, K., Hornák, K., Jezbera, J., Nedoma, J., Znachor, P., Hejzlar, J., Sed'a, J., 2008. Spatio-temporal patterns of bacterioplankton production and community composition related to phytoplankton composition and protistan bacterivory in a dam reservoir. Aqu. Microb. Ecol. 51, 249-262. doi: 10.3354/ame01193
- Smith, V. H., 2003. Eutrophication of freshwater and coastal marine ecosystems - A global problem. Env. Sci. Poll. Res. 10, 126-139. https://doi.org/10.1065/espr2002.12.142
- Song, H., Xu, J., Lavoie, M., Fan, X., Liu, G., Sun, L., … Qian, H., 2017. Biological and chemical factors driving the temporal distribution of cyanobacteria and heterotrophic bacteria in a eutrophic lake (West Lake, China). Appl. Microbiol. Biotech. 101(4), 1685-1696. doi: 10.1007/s00253-016-7968-8
- Sun, J., Liu, D., 2003. Geometric models for calculating cell biovolume and surface area for phytoplankton. J. Plankton Res. 25, 1331e1346. doi : 10.1093/plankt/fbg096.
- Talling, J., 1986. The seasonality of phytoplankton in african lakes. Hydrobiol. 138, 139-160. doi:10.1007/BF00027237.
- Teeling, H., Fuchs, B.M., Becher, D., Klockow, C., Gardebrecht, A., Bennke, C.M., … Amann, R., 2012. Substrate-controlled succession of marine bacterioplankton populations induced by a phytoplankton bloom. Science 336(6081), 608-611. doi: 10.1126/science.1218344.

- Wang, L.C., Zi, J.M., Xu; R.B., Hilt, S., Hou, X.L., Chang, X.X., 2017. Allelopathic effects of *Microcystis aeruginosa* on green algae and a diatom: evidence from exudates addition and co-culturing. Harmful Algae 61, 56-62. doi: 10.1051/limn/2019006
- Wickham, H., 2016. ggplot2: elegant graphics for data analysis. Springer-Verlag New York. ISBN 978-3-319-24277-4.
- Wilhelm, S.W., Bullerjahn, G.S., McKay, R.M.L., 2020. The complicated and confusing ecology of *Microcystis* blooms. MBio 11(3). doi: 10.1128/mBio.00529-20.
- Wood, S.N., 2011. Fast stable restricted maximum likelihood and marginal likelihood estimation of semiparametric generalized linear models. J. Royal Stat. Soc. (B) 73(1), 3-36. https://doi.org/10.1111/j.1467-9868.2010.00749.x
- Woodhouse, J.N., Ziegler, J., Grossart, H.-P., Neilan, B.A., 2018. Cyanobacterial community composition and bacteria–bacteria interactions promote the stable occurrence of particle-associated bacteria. Front. Microbio. 9, 777. doi: 10.3389/fmicb.2018.00777.
- Zhang, W., Zhou, Y., Jeppesen, E., Wang, L., Tan, H., Zhang, J., 2019. Linking heterotrophic bacterioplankton community composition to the optical dynamics of dissolved organic matter in a large eutrophic Chinese lake. Sci Total Environ 679, 136-147.
- Zhang, Z., Fan, X., Peijnenburg, W.J.G.M., Zhang, M., Sun, L., Zhai, Y., … Qian, H., 2021. Alteration of dominant cyanobacteria in different bloom periods caused by abiotic factors and species interactions. J. Env. Sci. 99, 1-9. doi: 10.1016/j.jes.2020.06.001.
- Zhou, J., Chen, G.-F., Ying, K.-Z., Jin, H., Song, J.-T., Cai, Z.-H., 2019. Phycosphere microbial succession patterns and assembly mechanisms in a marine dinoflagellate bloom. Appl. Environ. Microbiol. 85, e00349-19.

- Zhu, L., Zancarini, A., Louati, I., De Cesare, S., Duval, C., Tambosco, K., … Humbert, J.-F., 2016. Bacterial communities associated with four cyanobacterial genera display structural and functional differences: evidence from an experimental approach. Front. Microbiol. 7. doi: 10.3389/fmicb.2016.01662

Legends

Figure 1:

Temporal dynamic of Chl-*a* concentration, as well as the composition of phytoplankton community expressed as biovolume proportions (see Table S1 and S2 for more details). The three temporal phytoplanktonic stages (defined by the SIMPROF analyis, see Figure S1) are highlighted by the colored panels (stage I, green; stage II, red and stage III, blue).

Figures 2: Temporal dynamic of the microbial diversity indexes (boxplot representation of Richness, Inverse Simpson and Evenness indices), according to the three stages identified in the phytoplankton community (see Figures 1 and S1 for more details), within the Particle-associated (A) and the Free-living (B) fractions.

Figure 3: Redundancy analysis of the bacterial communities, based on a Bray-Curtis distance matrix for the PA (triangle) and FL (circle) communities. Colors indicate the three stages identified in the phytoplankton community (see Fig. 1). The values in brackets correspond to the percentages of the total variance information represented by each axis.

Figure 4: Temporal dynamic of the discriminating OTUs, that contributed to up to 70% of the dissimilarity between PA and FL communities (p-value <0.01) and for which a differential abundance was observed (Table S7). The abundances are expressed as relative abundance of the total reads, and presented in a heatmap. An overview of the phytoplankton dynamic (Figure 1) with the defined three stages is placed above the graphs.

745 **Figures 5**: Temporal dynamic of the discriminating OTUs, that contributed to up to 70% of the
746 dissimilarity within PA and FL communities separately (p-value <0.01) and for which a differential
747 abundance was observed among the 3 phytoplanktonic stages (Table S8). Three and four temporal
748 patterns were observed in the PA and FL fractions, respectively. The temporal patterns are
749 illustrated with the black frames. The abundances are expressed as relative abundance of the total
750 reads, and presented in a heatmap for (A) the particle-associated fraction and (B) the Free-living
751 fraction. The OTUs that contributed the most to the dissimilarity are highlighted by * symbols
752 (Table S8). An overview of the phytoplankton dynamic (Figure 1) with the defined three stages is
753 placed above the graphs.
754

Figure 1_R2

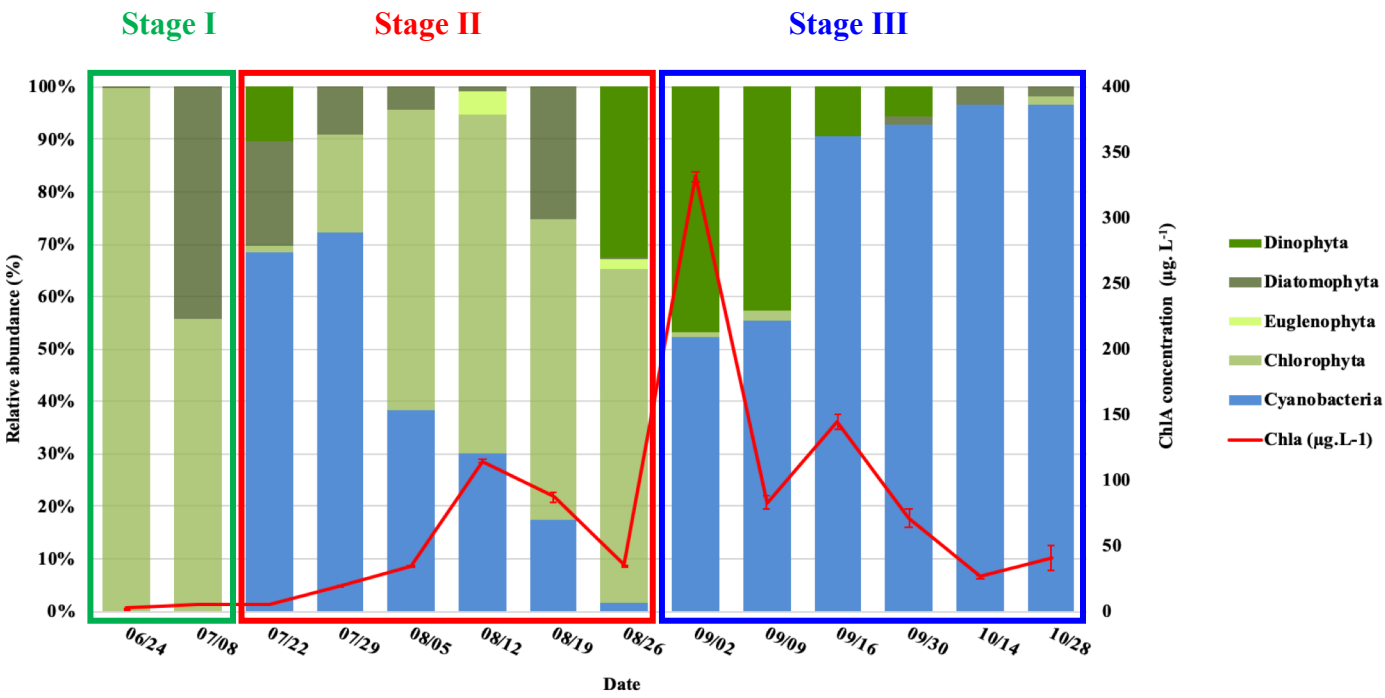
Stage I
Stage II
Stage III
Relative abundance (%)
100%
90%
80%
70%
60%
50%
40%
30%
20%
10%
0%
ChlA concentration (μg.L-1)
400
350
300
250
200
150
100
50
0
06/24
07/08
07/22
07/29
08/05
08/12
08/19
08/26
09/02
09/09
09/16
09/30
10/14
10/28
Date
Dinophyta
Diatomophyta
Euglenophyta
Chlorophyta
Cyanobacteria
Chla (μg.L-1)

Figures 2_R2

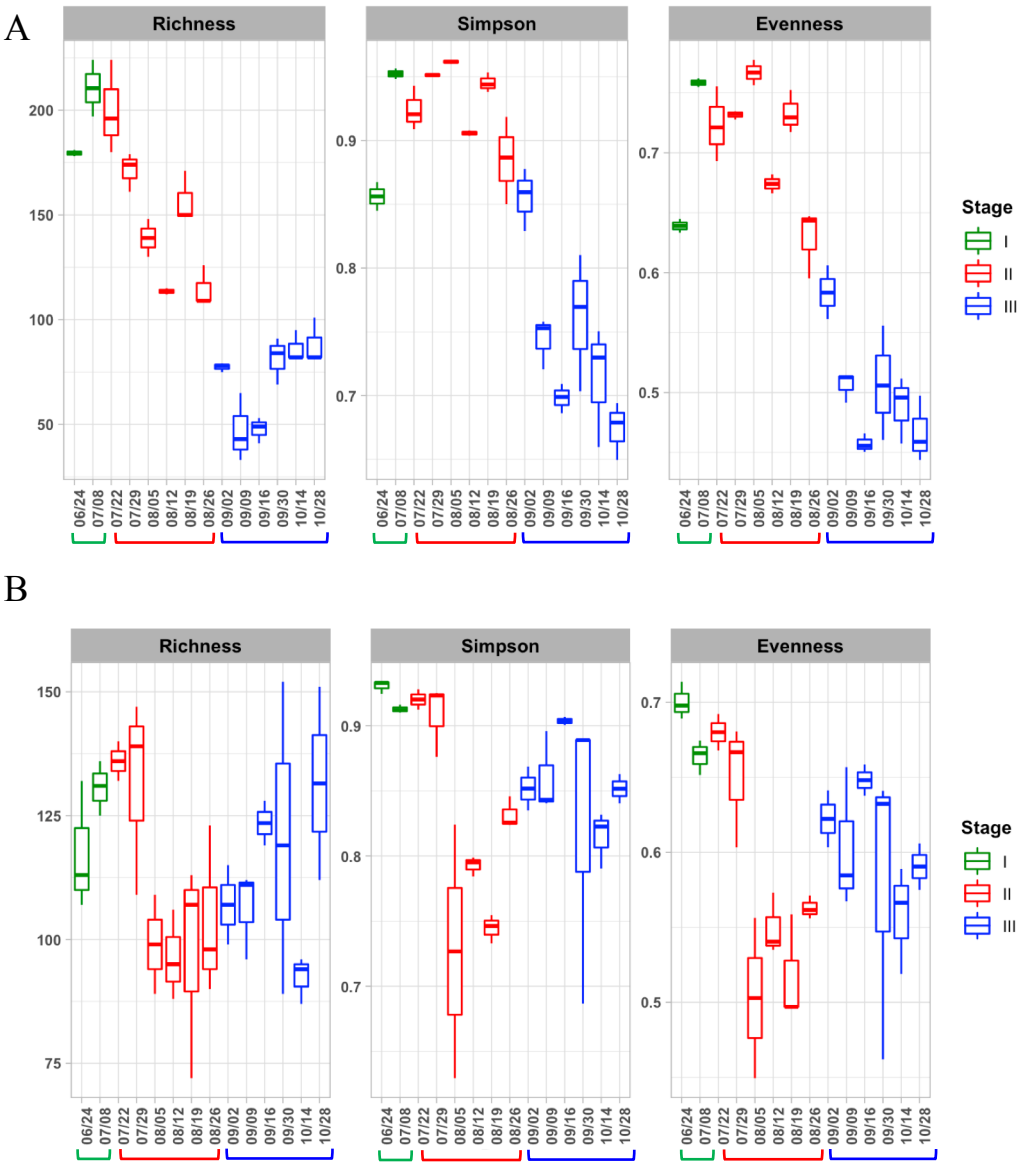
A
Richness
Simpson
Evenness
Stage
I
II
III
B
Richness
Simpson
Evenness
Stage
I
II
III

Figure 4_R2

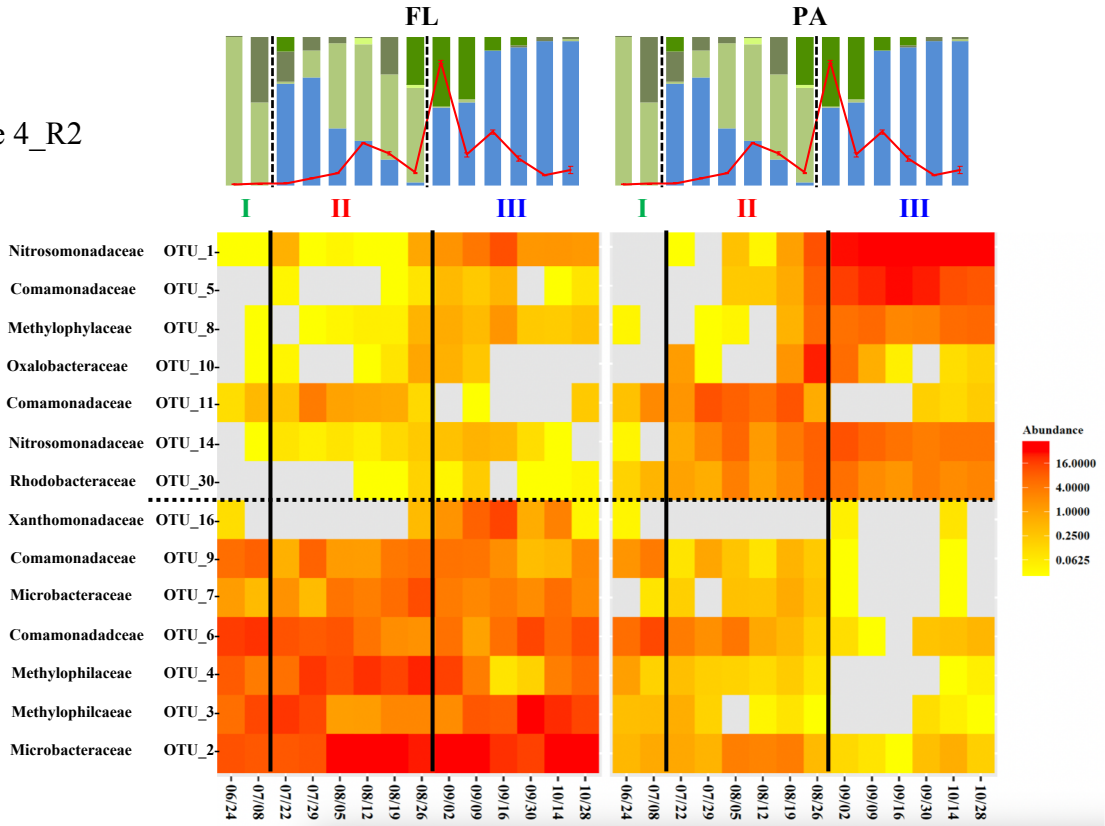

Figure 5_R2 Click here to access/download;Figure;Figure5AB_R2.pdf

Figures 5A and B

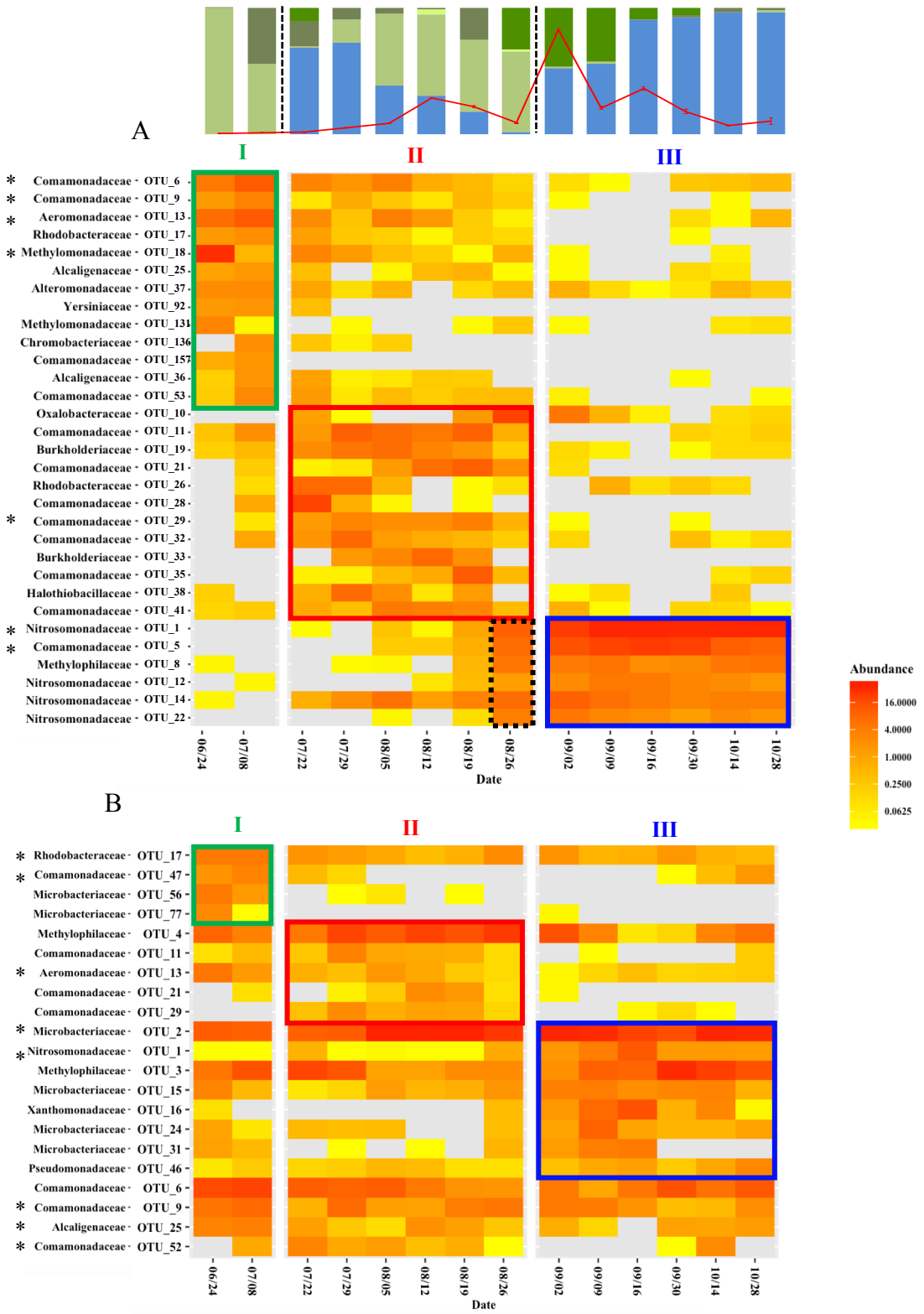

Supplementary file_1

Supplementary file_2

Click here to access/download

Supplementary Material

R2_Leloup_Supplemental_Information_2.docx

HARMFUL ALGAE

AUTHOR DECLARATION

Submission of an article implies that the work described has not been published previously (except in the form of an abstract or as part of a published lecture or academic thesis), that it is not under consideration for publication elsewhere, that its publication is approved by all authors and tacitly or explicitly by the responsible authorities where the work was carried out, and that, if accepted, it will not be published elsewhere in the same form, in English or in any other language, without the written consent of the copyright-holder.

By attaching this Declaration to the submission, the corresponding author certifies that:

- The manuscript represents original and valid work and that neither this manuscript nor one with substantially similar content under the same authorship has been published or is being considered for publication elsewhere.

- Every author has agreed to allow the corresponding author to serve as the primary correspondent with the editorial office, and to review the edited typescript and proof.

- Each author has given final approval of the submitted manuscript and order of authors. Any subsequent change to authorship will be approved by all authors.

- Each author has participated sufficiently in the work to take public responsibility for all the content.

Declaration of interests

☒ The authors declare that they have no known competing financial interests or personal relationships that could have appeared to influence the work reported in this paper.

☐The authors declare the following financial interests/personal relationships which may be considered as potential competing interests: